Available online at www.sciencedirect.com
ScienceDirect
Applied Catalysis B: Environmental 79 (2008) 110–116
APPLIED CATALYSIS B: ENVIRONMENTAL
www.elsevier.com/locate/apcatb

The effect of H_2O on the reduction of SO_2 and NO by CO on La_2O_2S

Ngai T. Lau *, Ming Fang, Chak K. Chan

Department of Chemical Engineering, The Hong Kong University of Science and Technology, Clear Water Bay, Hong Kong

Received 25 November 2006; received in revised form 3 October 2007; accepted 4 October 2007
Available online 7 October 2007

Abstract

The effect of H_2O on the catalytic reduction of SO_2 and NO on La_2O_2S was studied using temperature-programmed reaction coupled with fast mass spectrometry, powder X-ray diffraction and X-ray photoelectron spectroscopy. It is found that La_2O_2S can be completely and irreversibly deactivated in the presence of H_2O at 700 °C when NO/SO_2 is sufficiently high (~1.0). This is caused by the formation of a layer of inactive and stable $La_2O_2SO_4$ on the oxysulfide. When NO is absent or NO/SO_2 is low (~0.4), H_2O inhibits the reduction and shifts the selectivity from sulfur to H_2S. While the causes of the deactivation can be attributed to the Reverse Claus Reaction between H_2O and sulfur in the oxysulfide, the competitive hydrolysis of the COS intermediate and the competitive adsorption of H_2O, the shift in selectivity to H_2S is attributable to the former two factors.

Keywords: Lanthanum oxysulfide; Deactivation; Selectivity; Hydrogen sulfide; Hydrolysis

1. Introduction

SO_2 and NO are often produced simultaneously in combustion processes. Although there are scrubbing and oxidation treatment processes to remove these acid gases from flue gas, these processes usually produce a huge amount of products that need proper disposal. Catalytic reduction that simultaneously transforms these oxides to their elemental forms is desirable because it is simple and concentrates the pollutants into much smaller packages. A number of catalysts, mainly composite and supported transition metals such as Cu/Al_2O_3 [1], Fe/Al_2O_3 [2], Fe/Cr_2O_3 [3], Co, Mo, CoMo and FeMo supported on Al_2O_3 [4], Co/TiO_2 [5], SnO_2–TiO_2 solid solution [6] and transition metal-La_2O_2S [7] have been studied for the reduction. In particular, lanthanum oxysulfide (La_2O_2S), the active ingredient of the transition metal-La_2O_2S catalysts that are produced from lanthanum perovskite oxides and effective for the reduction of SO_2 [8,9], is the only material known to be highly active for the reduction of SO_2 [10] and the simultaneous reduction of SO_2 and NO [7] on its own without the participation of another material.

On the other hand, H_2O, a common ingredient of flue gas, is known to inhibit the reduction of SO_2 by CO on La_2O_2S and the selectivity is shifted from sulfur to H_2S [10]. The causes of these changes were attributed to the Reverse Claus Reaction between the product sulfur and H_2O, the competitive hydrolysis of the COS intermediate and the water–gas shift reaction. However, the impact of common deactivation factors such as sintering, competitive adsorption of H_2O and change in catalyst composition has not been evaluated. Moreover, the effect of H_2O on the simultaneous reduction of NO and SO_2 on La_2O_2S has also not been studied. This information is important in the development of a viable catalyst for the simultaneous removal of these acid gases.

There are many studies in the literature on the effect of H_2O on La_2O_3, the precursor of La_2O_2S. La_2O_3 has a structure close to La_2O_2S with the sulfide ion replaced by an oxide ion. de Asha et al. [11] and Paulidou and Nix [12] showed that H_2O is dissociatively adsorbed on La_2O_3 at room temperature. It is likely that La_2O_2S also adsorbs H_2O and the adsorption is dissociative. Toops et al. [13,14] studied the deactivation of competitive H_2O adsorption on La_2O_3 in the reduction of NO and found that La_2O_3 was deactivated in the presence of SO_2 and $La_2O_2SO_4$ was formed on the oxide [13].

It has been shown that the reduction of SO_2 by CO on La_2O_2S follows the COS intermediate mechanism [10,15,16],

* Corresponding author. Tel.: +852 2358 6935; fax: +852 2719 6710.
E-mail address: ntlau@ust.hk (N.T. Lau).

0926-3373/$ – see front matter © 2007 Elsevier B.V. All rights reserved.
doi:10.1016/j.apcatb.2007.10.004

which can be represented by the following reaction steps:

$$CO + S \rightarrow COS, \quad (1)$$

$$SO_2 + 2COS \rightarrow 3S + 2CO_2, \quad (2)$$

where S is labile sulfur in the oxysulfide. It can be formed by the reduction of SO_2 or comes from the lattice when the oxysulfide is heated [15].

$$*S \rightarrow S + *, \quad (3)$$

where '*' is an anion vacancy. Reaction (2) is accomplished on La_2O_2S probably via the surface reaction between COS and pools of SO_2 adspecies [16]. Rare earth oxysulfides are highly catalytically active for the hydrolysis of COS to H_2S [17].

For the reduction of NO on La_2O_2S, it has been shown that the reduction probably starts with decomposition of NO to N and O at the anion vacancies [18]. The labile sulfur in the oxysulfide removes O as SO_2 to regenerate the vacancies while N desorbs as N_2. The SO_2 produced is then reduced by CO to sulfur once again on La_2O_2S and this reduction reaction maintains the population of sulfur in the oxysulfide.

It is clear that sulfur plays an essential role in both the reduction of SO_2 and NO. Any interaction between H_2O and the sulfur species would have enormous influences on the reduction reactions. Since the reduction of NO consumes sulfur while the reduction of SO_2 replenishes the oxysulfide with sulfur, the relative amount of NO to SO_2 is expected to be critical to these reduction reactions in the presence of H_2O.

We report here the effect of H_2O on the reduction of SO_2 and the simultaneous reduction of NO and SO_2 by CO on La_2O_2S and, in particular, the impact of H_2O on the surface sulfur species and the COS intermediate, and the influence of the NO/SO_2 ratio on the simultaneous reduction reaction. The changes in the bulk and surface composition of the catalyst due to these reduction reactions in the presence of H_2O are also reported.

2. Experimental

2.1. Catalyst preparation

La_2O_2S was synthesized in situ in the quartz microreactor from $La(OH)_3$ powder (Yiaolong, China) using the sulfidization procedure reported by Ma et al. [19] at 700 °C for 3 h. The oxysulfide was then kept in flowing Ar inside the reactor before use. The composition of the synthesized samples was confirmed to be La_2O_2S using powder X-ray diffraction (XRD). The typical XRD diffractogram of these La_2O_2S samples is shown in Fig. 1. The specific surface area of these samples was approximately 4 $m^2\ g^{-1}$, which was comparable to the reported value [19].

2.2. TPR/MS

TPR/MS study was performed with the experimental setup shown in Fig. 2. A humidifier was used to moisturize the Ar stream at room temperature. About 0.1 g La_2O_2S was synthesized in situ in the microreactor. The feed gas at

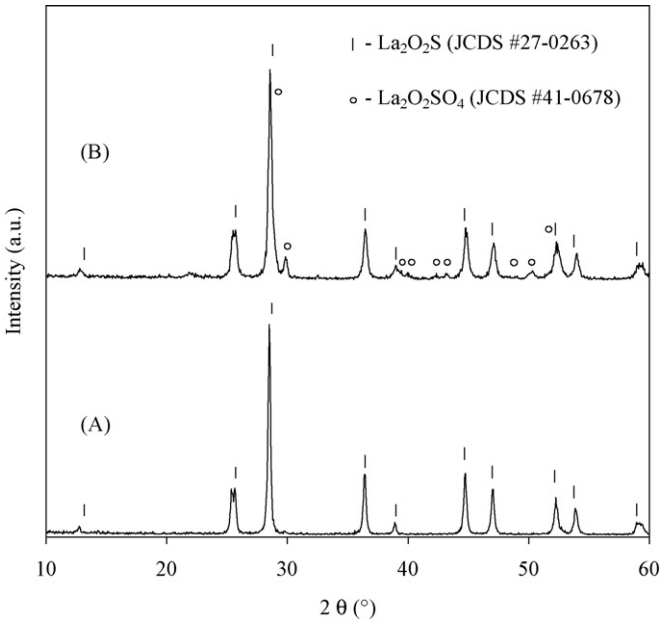

Fig. 1. XRD diffractogram: (A) La_2O_2S as synthesized and (B) formation of $La_2O_2SO_4$ after the reduction of NO and SO_2 at NO/SO_2 = 1 in the presence of H_2O.

100 ml min^{-1} at room temperature (~25 °C) was obtained by mixing the Ar stream and preblended reaction gases at the gas mixing flask before it was fed to the reactor. The composition of the effluent gas from the reactor was continuously monitored by the mass spectrometer MS250 (EXTREL), which reported the composition every second. The typical composition of the feed gases was:

(C1) 0.4 vol.% SO_2 and 0.8 vol.% CO
(C2) 0.16 vol.% NO, 0.4 vol.% SO_2, 0.96 vol.% CO (NO/SO_2 = 0.4)
(C3) 0.4 vol.% NO, 0.4 vol.% SO_2, 0.96 vol.% CO (NO/SO_2 = 1.0)
(C4) 0.4 vol.% SO_2, 0.8 vol.% CO and 2.9 vol.% H_2O
(C5) 0.16 vol.% NO, 0.4 vol.% SO_2, 0.96 vol.% CO and 2.9 vol.% H_2O (NO/SO_2 = 0.4)
(C6) 0.4 vol.% NO, 0.4 vol.% SO_2, 0.96 vol.% CO and 2.9 vol.% H_2O (NO/SO_2 = 1.0)

The TPR temperature program started with purging the La_2O_2S sample with the feed gas at room temperature until the composition of the effluent gas became steady. Then the sample was heated from room temperature to 700 °C at 10 °C min^{-1} and kept at 700 °C for 2 h or until the composition of the effluent gas became steady again.

2.3. Catalyst composition

The changes in the bulk and surface composition of La_2O_2S due to the reduction reactions in the presence of H_2O were monitored with XRD and XPS (X-ray photoelectron spectroscopy). The as-sulfidized La_2O_2S was used as the reference. The XRD analysis was performed with the Powder X-ray

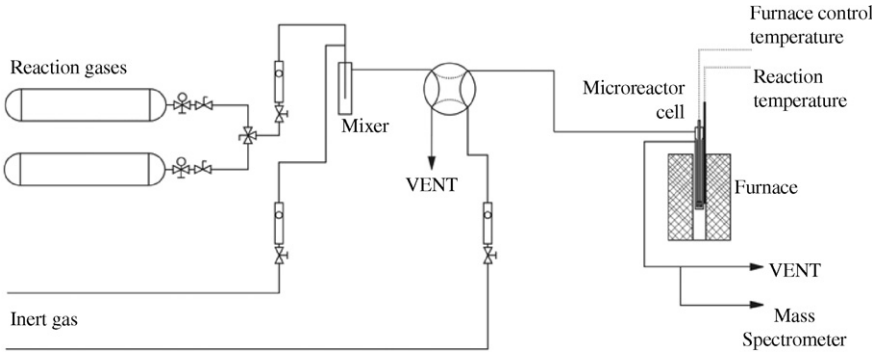

Fig. 2. Flow schematic of the experimental setup.

Diffraction System (Model PW1830, PHILIPS) operated at 2 kW using Cu-anode and graphite monochromator. The samples were spread and pressed onto glass sample holders with no pretreatments.

The XPS analysis was performed with Perkin-Elmer Surface Science Analysis System (Model PHI 5600) using monochromatic Al Kα X-ray source according to the procedure described by Lau and Fang [15]. The powder samples were pressed into cup-shaped sample mounts for direct insertion into the instrument. Low energy flooding electrons were used to neutralize the charges built up on the samples and the binding energy (BE) scale was so adjusted to make the adventitious carbon peak at 284.5 eV. Multiplex scans of carbon C 1s, nitrogen N 1s, oxygen O 1s, sulfur S 2p and lanthanum La 3d were acquired at constant pass energy of 23.5 eV.

3. Results

3.1. Change in catalyst composition

In general, XRD did not find any significant changes in the bulk composition of the catalyst samples after the reactions. The only exception is the sample used in the reduction of NO and SO_2 at high NO/SO_2 (1.0) in the presence of H_2O, a small but significant amount of $La_2O_2SO_4$ was found (curve B, Fig. 1). On the other hand, XPS revealed changes in the surface composition of the samples when H_2O was involved. The XPS O 1s and S 2p spectra of these samples are showed in Fig. 3 alongside with the as-sulfidized La_2O_2S as reference. The XPS spectra of the as-sulfidized sample are close to those reported by Lau and Fang [15]. Typical C ls, O 1s and S 2p peaks are listed in Table 1 and the surface concentration of carbon, oxygen and sulfur species, in ratios to La, of the La_2O_2S samples are listed in Table 2. In general, the O 1s spectrum consists two peaks—one at ~529 eV due to oxide and the other at higher BE attributable to the oxygen bonded to sulfur and carbon. The S 2p also contains two modes—the sulfide peak, possibly including the adsorbed sulfur, at ~160 eV and a group of S–O (sulfur–oxygen species such as SO_2 adspecies, sulfite and sulfate) peaks at 166–169 eV. Lastly, no detectable amount of nitrogen was found in the surface of the catalysts used in the reduction of NO.

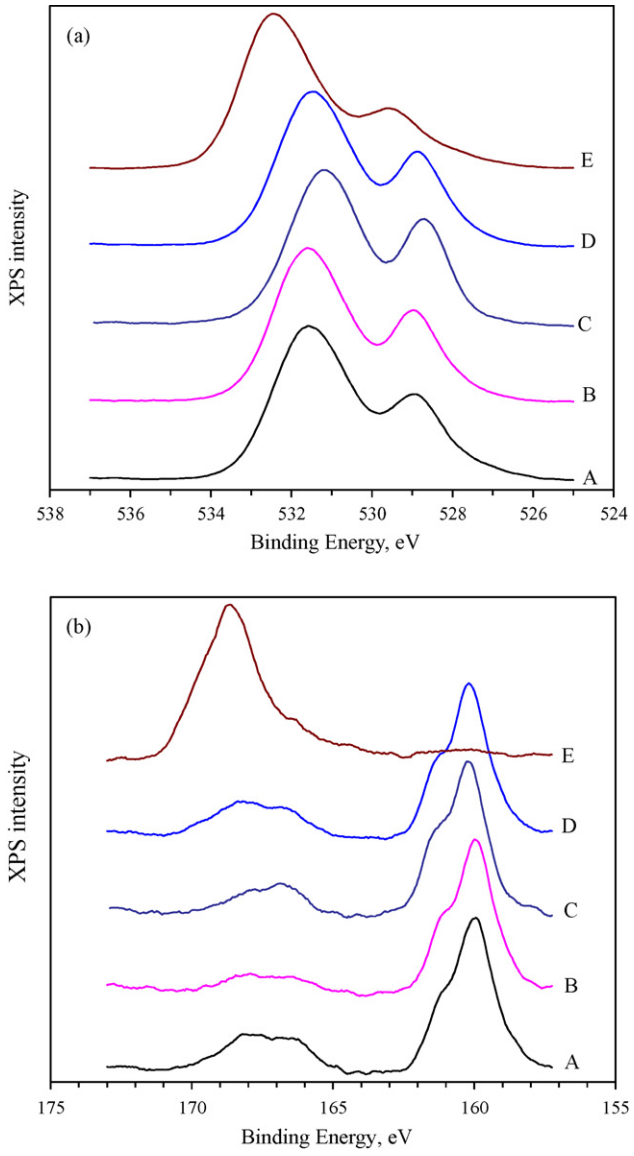

Fig. 3. XPS spectra (a) O 1s and (b) S 2p of La_2O_2S for SO_2 reduction–effect of H_2O. Curves from bottom to top: (A) as-sulfidized, (B) as-hydrolyzed, (C) after COS + H_2O reaction, (D) after SO_2 + CO + H_2O reaction and (E) NO + SO_2 + CO + H_2O reaction. All spectra are normalized to the same intensity span.

Table 1
Typical XPS C 1s, O 1s and S 2p of La_2O_2S for SO_2 reduction–effect of H_2O

Reaction treatment	C 1s (eV)		O 1s (eV)		S 2p (eV)	
	AC	C–O			Sulfide	S–O
(A) As-sulfidized	284.5	289.1	531.5	528.9	160.0	166.4–168.0
(B) As-hydrolyzed	284.5	289.2	531.5	528.9	160.0	166.3–167.9
(C) $COS + H_2O$	284.5	289.0	531.1	528.7	160.1	166.5–167.8
(D) $SO_2 + CO + H_2O$	284.5	289.1	531.4	528.8	160.1	166.5–168.2
(E) $NO + SO_2 + CO + H_2O$ ($NO/SO_2 = 1.0$)	284.5	289.0	532.4	529.5	–	168.6

AC stands for adventitious carbon (284.5 eV). La_2O_2S samples were produced using sulfidization method with a stoichiometric mixture of SO_2 and CO. AC = adventitious carbon, C–O = carbon species with oxygen such as carbonate, and S–O = sulfur species with oxygen such as SO_2 adspecies, sulfite and sulfate.

Table 2
Changes in the concentration of surface carbon, oxygen and sulfur in La_2O_2S due to the reduction of SO_2 in the presence of H_2O

Reaction treatment	C/La	O/La	S/La	S_{ONLY}/La	S–O/La
(A) As-sulfidized	1.3	3.2	0.65	0.46	0.20
(B) As-hydrolyzed	1.6	3.0	0.46	0.38	0.08
(C) $COS + H_2O$	1.6	3.0	0.67	0.54	0.13
(D) $SO_2 + CO + H_2O$	1.2	3.0	0.55	0.43	0.12
(E) $NO + SO_2 + CO + H_2O$ ($NO/SO_2 = 1.0$)	1.0	4.5	0.70	0.02	0.68

C/La, O/La and S/La are the atomic ratio of carbon, oxygen and sulfur to lanthanum in the surface. S_{ONLY} is those surface sulfur species that are not bonded to oxygen such as sulfide and sulfur adsorbed on the oxysulfide, while S–O is the surface sulfur species that are bonded with oxygen.

Among the various H_2O reactions, the hydrolysis of La_2O_2S most severely depleted the surface sulfur species in the oxysulfide. Reducing SO_2 in the presence of H_2O gave similar but smaller depletion of sulfur. When COS was present (hydrolysis of COS on La_2O_2S), a significantly higher concentration of these sulfur species was maintained in the surface possibly due to the constant supply of sulfur from COS. However, in all cases, the concentration of S–O, the sulfur species bonded to oxygen, significantly decreased. This suggests that S–O species such as SO_2 adspecies were being displaced by H_2O in competitive adsorption.

The reduction of NO at $NO/SO_2 = 1.0$ in the presence of H_2O significantly increased the surface concentration of oxygen and sulfur, in which S–O species almost completely dominated the surface sulfur content (see Fig. 3b and Table 2). In particular, the sample had La $3d_{5/2}$ peaks at 833.7 eV and 838.0 eV, S 2p at 168.6 eV, and O 1s at 529.5 eV and 532.4 eV. These peaks are comparable to Aono et al. [20], who reported La $3d_{5/2}$ at 834.01 eV, S 2p at 168.77 eV, and O 1s at 528.77 eV for lattice oxygen and 531.75 eV for S–O on lanthanum oxysulfate ($La_2O_2SO_4$) with the adventitious carbon set at 284.5 eV. Thus, combining with the XPS and XRD results, it is certain that a layer of $La_2O_2SO_4$ was formed on the surface of the oxysulfide.

3.2. TPR/MS

3.2.1. Deactivation and shift in selectivity

In the presence of H_2O, La_2O_2S became completely and irreversibly deactivated at 700 °C when NO/SO_2 was large (~1.0). No H_2S was found in the effluent gas. Removing H_2O from the feed did not reactivate the sample. When NO was absent or when NO/SO_2 was small (~0.4), La_2O_2S was partially deactivated. Table 3 shows clearly that the conversions of SO_2 and NO were lowered significantly in the reduction of SO_2 and simultaneous reduction of SO_2 and NO, when H_2O was present. Besides, the reduction in the conversion of SO_2 was more than that of NO.

Figs. 4a and 5a are the temporal TPR/MS profiles for the reduction of SO_2 and simultaneous reduction of NO and SO_2 in the presence of H_2O. The respective thermal TPR/MS profiles for these reactions when H_2O was removed from the feed are in Figs. 4b and 5b. The conversion C is computed with the following equation:

$$C = \frac{I_O - I}{I_O}, \quad (4)$$

where I_O and I are the intensities of the selected mass fragments of reactant species in the feed and effluent streams, respectively. The major mass fragments of H_2O, CO, NO, H_2S, CO_2, COS and SO_2 are m/z = 18, 28, 30, 34, 44, 60 and 64, respectively. The formation of N_2 (same m/z as CO) from the reduction of NO can interfere with the measurement of CO and thus can apparently lower the conversion. This explains why the conversion of CO is significantly lower than both of NO and SO_2 in

Table 3
Comparison of conversions of NO and SO_2 in the presence and absence of H_2O for the reduction of NO and SO_2 at 700 °C on La_2O_2S

Reaction	With H_2O (%)		Without H_2O (%)	
	SO_2	NO	SO_2	NO
$SO_2 + CO$	70	–	91[a]	–
$NO + SO_2 + CO$ ($NO/SO_2 = 0.4$)	54	92	94	99

[a] Reduction of SO_2 on La_2O_2S which was subjected to hydrolysis treatment in the previous TPR run.

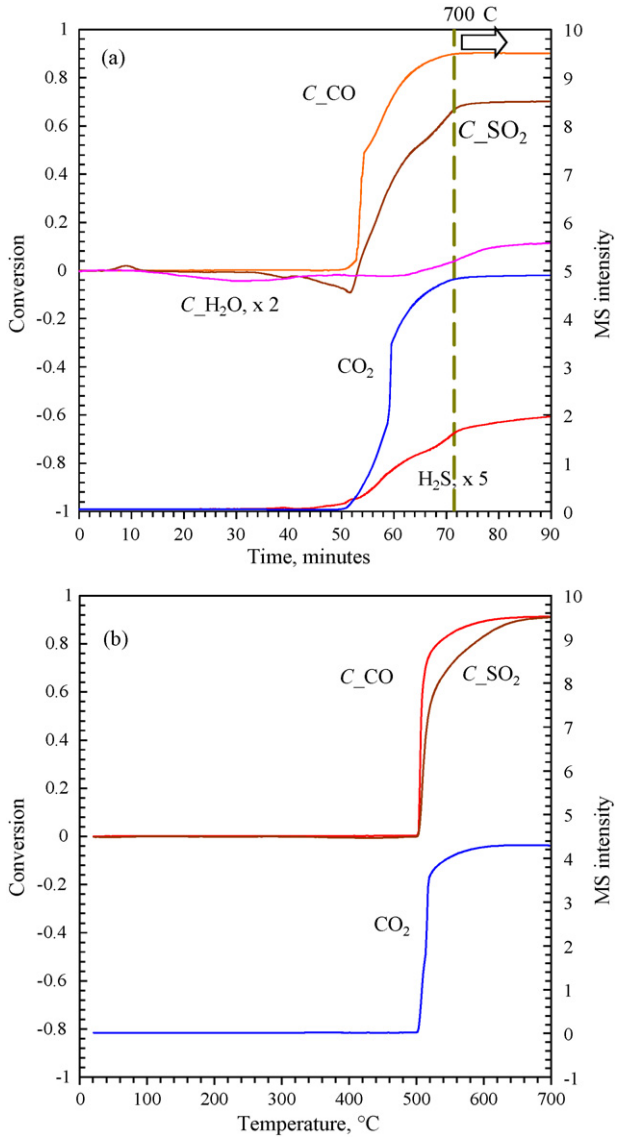

Fig. 4. Reduction of SO_2 by CO on La_2O_2S in the (a) presence and (b) absence of H_2O. (a) Plotted on time scale while (b) on temperature scale. (b) Shows the reduction of SO_2 on La_2O_2S which has been hydrolyzed in the last TPR run. C_{H_2O}, C_{CO} and C_{SO_2} are conversion curves of H_2O, CO and SO_2 based on the intensity m/z = 18, 28 and 64, respectively (left *Y*-axis). The remaining curves are the mass intensities for H_2S (m/z = 34) and CO_2 (m/z = 44) (right *Y*-axis). The dashed line in (a) marks the beginning of the 700 °C soaking step. The H_2S intensity is scaled up by 5 and C_{H_2O} by 2.

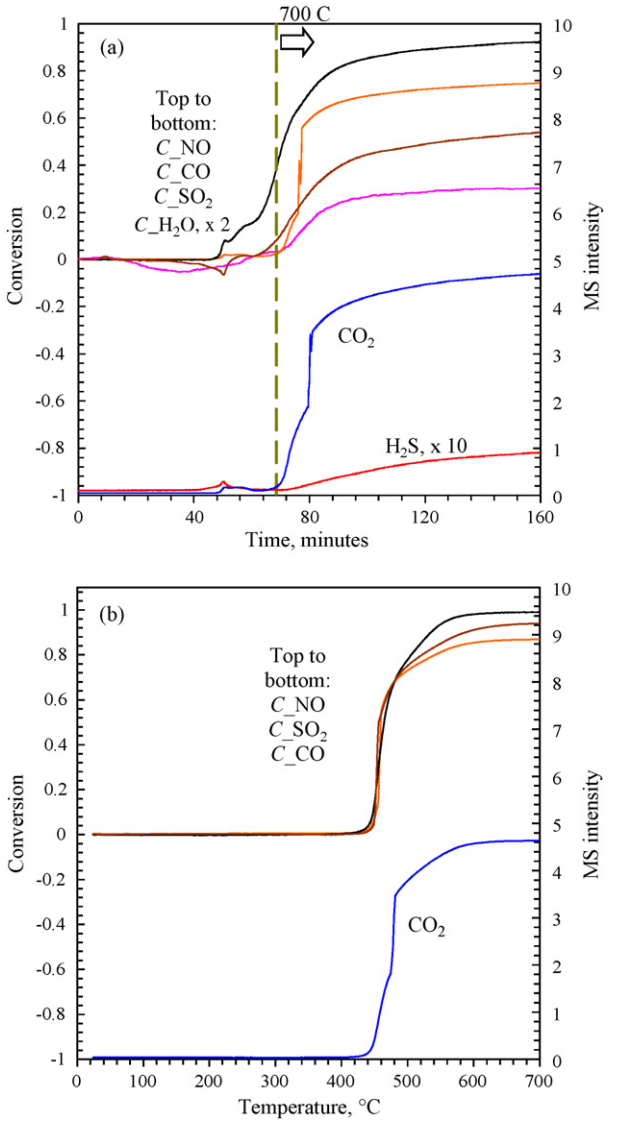

Fig. 5. Reduction of NO and SO_2 by CO on La_2O_2S at NO/SO_2 = 0.4 in the (a) presence and (b) absence of H_2O. (a) is plotted on time scale while (b) is plotted on temperature scale. C_{H_2O}, C_{NO} and C_{SO_2} traces are the conversion of H_2O, NO and SO_2, and based on the intensity m/z = 18, 30 and 64, respectively. C_{CO} (m/z = 28) is the sum of the consumption of CO and formation of N_2. The CO_2 (m/z = 44) intensity curve traces the sum of the formation of CO_2 and N_2O. Left *Y*-axis is conversion and right *Y*-axis is the intensity. The dashed line in (a) marks the beginning of the 700 °C soaking step. The H_2S (m/z = 34) intensity is scaled up by 10 and C_{H_2O} by 2.

the reduction of NO and SO_2 (Fig. 5). On the other hand, the measurement of H_2O is not affected by the mass fragments of other reaction species. More detailed discussions on this computation can be found in our previous publication [18]. It can be seen that the reduction reactions started sluggishly with higher ignition temperatures and the conversions of NO, SO_2 and CO were lower than those in the absence of H_2O at the same temperature. In addition, as SO_2 was reduced by CO in the presence of H_2O, a significant amount of H_2S was produced.

3.2.2. *Hydrolysis of La_2O_2S*

Fig. 6 shows the thermal TPR/MS profile of the hydrolysis of La_2O_2S. At >320 °C, both H_2S and SO_2 were produced and their profiles were close. The concentration of the sulfur not bonded to oxygen (S_{ONLY}/La) in the surface decreased significantly after hydrolysis (see Table 2). These results suggest the occurrence of the Reverse Claus Reaction between H_2O and sulfur in the oxysulfide.

$$2H_2O + 3S \rightarrow SO_2 + 2H_2S. \quad (5)$$

The H_2S and SO_2 profiles are comparable to the COS formation profile on La_2O_2S reported by Lau and Fang [15]. The SO_2 and H_2S peaks at ~380 °C are due to the reaction between H_2O and labile sulfur in the surface of La_2O_2S. The formation of SO_2 and H_2S at higher temperatures are attributed

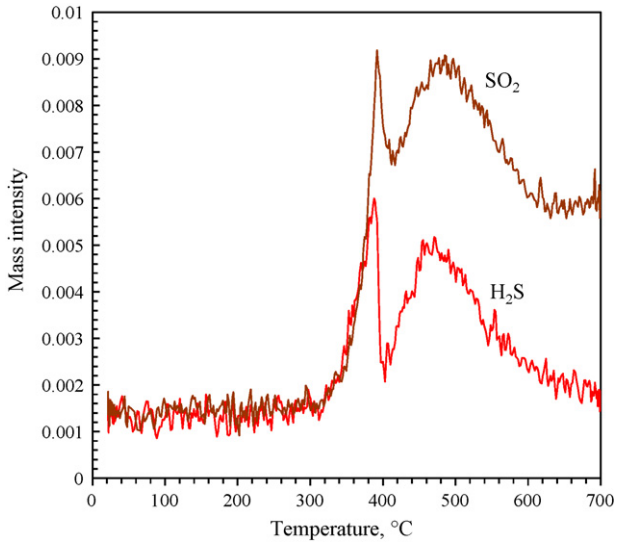

Fig. 6. Hydrolysis of La_2O_2S.

to the reaction between H_2O and lattice sulfur in the surface of the oxysulfide.

Even though SO_2 was produced in the hydrolysis, the concentration of the surface S–O (S–O/La) decreased (see Table 2). This suggests that H_2O hindered the adsorption of SO_2 on La_2O_2S but promoted desorption. The surface oxygen content increased with an increase in the relative intensity of the O 1s peak at ~528.9 eV, indicating that the concentration of the oxygen that was not bonded to sulfur and carbon such as lattice oxide and the adsorbed oxygen increased. As the sulfide ions in the surface lattice were removed by the hydrolysis, the surface of the oxysulfide was probably 'oxidized' to the oxide as the lattice sulfide was replaced by the oxide or hydroxide ions. This is supported by the TPR/MS result in Fig. 4b. When CO and SO_2 in stoichiometric ratio ($CO/SO_2 = 2$) started to react on

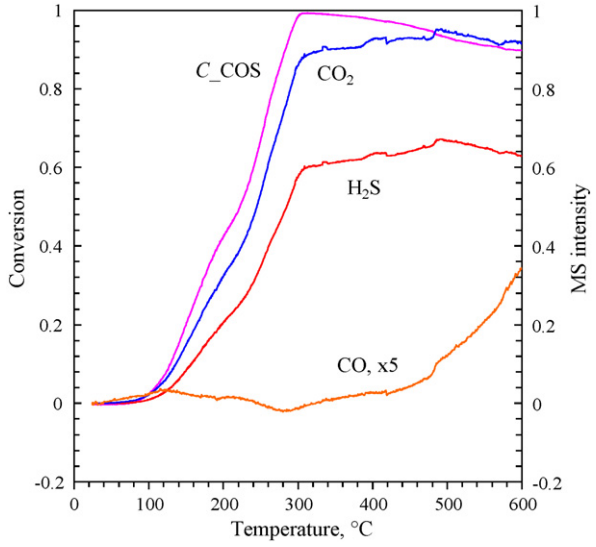

Fig. 7. Hydrolysis of COS on La_2O_2S. C_{COS} is the conversion curve of COS based on the intensity $m/z = 60$ (left *Y*-axis). The remaining curves are the mass intensities for CO ($m/z = 28$), H_2S ($m/z = 34$) and CO_2 ($m/z = 44$) (right *Y*-axis). The CO intensity is scaled up by 5.

La_2O_2S, more CO than SO_2 stoichiometrically was consumed to remove and convert the oxide/hydroxide to oxysulfide. Additional CO was needed to remove oxygen from the La_2O_3 lattice in the following transformation:

$$La_2O_3 + 3CO + SO_2 \rightarrow La_2O_2S + 3CO_2. \quad (6)$$

3.2.3. Hydrolysis of COS

La_2O_2S readily catalyzes the hydrolysis of COS to H_2S (Reaction (7)) with the concomitant formation of CO_2 (see Fig. 7). Almost complete conversion of COS was attained at 310 °C. This is comparable to that reported by Zhang et al. [17] on rare earth oxysulfides.

$$COS + H_2O \rightarrow H_2S + CO_2. \quad (7)$$

The drop in conversion at >310 °C can be attributed partly to catalyst sulfation [21], which is a common cause of deactivation for COS hydrolysis catalysts, and partly to the increasing decomposition of COS to CO at higher temperatures.

$$COS \rightarrow CO + S. \quad (8)$$

4. Discussions

4.1. Causes of deactivation

4.1.1. Case of the completely deactivated La_2O_2S

The complete and irreversible deactivation of La_2O_2S in the reduction of NO by CO at $NO/SO_2 = 1.0$ in the presence of H_2O can be attributed to the formation of a $La_2O_2SO_4$ layer on the surface. $La_2O_2SO_4$ is inactive for the reduction of NO and SO_2 by CO and is stable at typical reduction reaction conditions. This oxysulfate is known to decompose in air to oxide at temperatures >1000 °C [22]. Removing H_2O from feed does not reactivate the catalyst at typical reaction conditions. Toops et al. [13] reported that the formation of $La_2O_2SO_4$ was a cause of deactivation for La_2O_3 in the reduction of NO in the presence of SO_2.

4.1.2. Case of the partially deactivated La_2O_2S

The Reverse Claus Reaction (Reaction (5)) not only competes for labile sulfur with the reduction of SO_2 and NO, hinders the formation of the intermediate COS, inhibits the removal of the oxygen left from the decomposition of NO, but also oxidizes the sulfur in the oxysulfide back to SO_2, a detriment for the catalytic reduction. All these contribute to the loss of catalyst activity. Furthermore, the ability that H_2O oxidizes sulfur in the oxysulfide to SO_2 further promotes the formation of sulfur oxides such as SO_2 and sulfate, which are already favorably formed by the reactions with NO on La_2O_2S. In excess NO ($NO/SO_2 = 1.0$) atmosphere, the combined effect of NO and H_2O can be responsible for the formation of $La_2O_2SO_4$, which in turn completely deactivates the catalyst. In addition, H_2O can also react with the sulfur in the surface lattice, converting the surface of the oxysulfide to oxide/hydroxide.

In the presence of H_2O, COS is readily hydrolyzed to H_2S. COS is the reaction intermediate for the reduction of SO_2 on La_2O_2S. Although H_2S reacts with SO_2 through the Claus Reaction,

$$2H_2S + SO_2 \rightarrow 3S + 2H_2O, \quad (9)$$

this reaction is not so effective to convert SO_2 to sulfur as that between COS and SO_2 (Reaction (2)) at the SO_2 reduction temperature because the Claus Reaction is not favored at such high temperature [21]. The activity of La_2O_2S for the reduction of SO_2 is impaired. At the same time, COS is also an effective reducing agent for converting NO to N_2 on La_2O_2S [7]. The hydrolysis reaction reduces the concentration of COS that is available for the reduction of NO.

As the La_2O_2S catalysts were heated in the moisturized SO_2 reduction stream (Feed C4) and SO_2 and NO reduction stream (Feed C5), negative consumption of H_2O was found when SO_2 (Fig. 4a), and NO and SO_2 (Fig. 5a) started to be reduced. This suggests that a significant amount of H_2O could be desorbed from the La_2O_2S when the catalyst was heated to the reaction temperature. This also shows that the adsorption of H_2O is significant even in the presence of NO and SO_2. Since H_2O promotes the desorption of SO_2, it inhibits the reduction of SO_2 through competitive adsorption and interferes with the supply of sulfur needed for the NO reduction. Furthermore, the adsorption of H_2O on La_2O_2S possibly involves anion vacancies, which are responsible for the reduction of NO [18], and competes with the reduction for vacancies.

Sintering is a common cause of deactivation for catalysts, but it can be ruled out as a significant cause in this case due to the following reasons. First, sintering is a high temperature process. It is usually slow and occurs in materials with high specific surface area. Second, the melting point of La_2O_2S is 1940 °C [23], much higher than the catalyst manufacturing and operation temperature of 700 °C and the specific surface area of our samples is only 4 $m^2\ g^{-1}$. Third, the reaction time for the TPR run at slightly more than 3 h is short.

5. Shift in selectivity

The shift in selectivity from sulfur to H_2S is attributable to, first, the Reverse Claus Reaction between H_2O and sulfur in La_2O_2S and, second, the competitive hydrolysis of COS. Both reactions effectively convert sulfur and COS to H_2S while at 700 °C, the Claus Reaction becomes ineffective in removing H_2S, resulting in a substantial amount of H_2S left in the effluent. Hence, the reaction between H_2S and NO on La_2O_2S can play a significant role in the NO reduction reaction when H_2O is present. Further investigation on this H_2S reaction is warranted.

6. Conclusions

In this study, the effect of H_2O on the catalytic reduction of SO_2 and NO on La_2O_2S has been investigated using TPR/MS, XRD and XPS. It is found that La_2O_2S can be completely and irreversibly deactivated at 700 °C in the presence of H_2O when NO/SO_2 is sufficiently high (∼1.0). The cause of the deactivation is attributable to the formation of a layer of inactive and stable $La_2O_2SO_4$ on the oxysulfide. When NO is absent or NO/SO_2 is low (∼0.4), H_2O inhibits the reduction reactions on La_2O_2S and shifts the selectivity from sulfur to H_2S. The deactivation can be attributed to the Reverse Claus Reaction between H_2O and sulfur in the oxysulfide, the competitive hydrolysis of the COS intermediate and the competitive adsorption of H_2O. The shift in selectivity to H_2S is caused by the Reverse Claus Reaction and hydrolysis of the COS intermediate. It is critical to keep NO/SO_2 sufficiently low in order to avoid the complete and irreversible deactivation of La_2O_2S in the presence of H_2O.

Acknowledgement

This work was supported by the Research Grant Council of the Hong Kong Special Administration Region, China (Project No. HKUST6001/01P).

References

[1] C.W. Quinlan, V.C. Okay, J.R. Kittrell, Ind. Eng. Chem. Process Des. Dev. 12 (1973) 359.
[2] V.N. Goetz, A. Sood, J.R. Kittrell, Ind. Eng. Chem. Prod. Res. Dev. 13 (1974) 110.
[3] A. Sood, J.R. Kittrell, Ind. Eng. Chem. Prod. Res. Dev. 13 (1974) 180.
[4] S. Zhuang, M. Yamazaki, K. Omata, Y. Takahashi, M. Yamada, Appl. Catal. B: Environ. 31 (2001) 133.
[5] Z. Zhang, J. Ma, X. Yang, J. Mol. Catal. A: Chem. 195 (2003) 189.
[6] Z. Zhang, J. Ma, X. Yang, Chem. Eng. J. 95 (2003) 15.
[7] J. Ma, M. Fang, N.T. Lau, Catal. Lett. 62 (1999) 127.
[8] D.B. Hibbert, Catal. Rev. Sci. Eng. 34 (1992) 391.
[9] J. Ma, M. Fang, N.T. Lau, in: G. Centi, C. Cristiani, S. Perathoner, P. Forzatti (Eds.), Environmental Catalysis - For a better world and life: Proceedings of the 1st World Conference, SCI Pub., Rome (Italy), 1995, p. 555.
[10] J. Ma, M. Fang, N.T. Lau, Appl. Catal. A: Gen. 150 (1997) 253.
[11] A.M. de Asha, J.T.S. Critchley, R.M. Nix, Surf. Sci. 405 (1998) 201.
[12] A. Paulidou, R.M. Nix, Surf. Sci. 470 (2000) L104.
[13] T.J. Toops, A.B. Walters, M.A. Vannice, Appl. Catal. B: Environ. 38 (2002) 183.
[14] T.J. Toops, A.B. Walters, M.A. Vannice, J. Catal. 214 (2003) 292.
[15] N.T. Lau, M. Fang, J. Catal. 179 (1998) 343.
[16] N.T. Lau, M. Fang, C.K. Chan, J. Mol. Catal. A: Chem. 203 (2003) 221.
[17] Y. Zhang, Z. Xiao, J. Ma, Appl. Catal. B: Environ. 48 (2004) 57.
[18] N.T. Lau, M. Fang, C.K. Chan, J. Catal. 245 (2007) 301.
[19] J. Ma, M. Fang, N.T. Lau, J. Catal. 163 (1996) 271.
[20] H. Aono, M. Sakamoto, Y. Sadaoka, J. Ceram. Soc. Jpn. 108 (12) (2000) 1052.
[21] A. Piéplu, O. Saur, J. Lavalley, Catal. Rev. – Sci. Eng. 40 (4) (1998) 409.
[22] L. Niinistö, M. Leskelä, in: K.A. Gschneidner, Jr., L. Eyring (Eds.), Handbook on the Physics and Chemistry of Rare Earths, vol. 9, Elsevier Science Publishers B.V., North-Holland, Amsterdam, 1987, p. 91.
[23] J.M. Macintyre, F.M. Daniel, V.M. Stirling, first ed., Dictionary of Inorganic Compounds, vol. 3, Chapman & Hall, London: New York, 1992, p. 3549.